Process characteristics of fibre-laser-assisted plasma arc welding

A Mahrle, M Schnick, S Rose, C Demuth, E Beyer, U Füssel

Process characteristics of fibre-laser assisted plasma arc welding

A Mahrle[1], M Schnick[1], S Rose[1], C Demuth[1], E Beyer[1,2] and U Füssel[1]
[1]Dresden University of Technology, Institute of Surface and Manufacturing Technology, PO Box, D-01062 Dresden, Germany
[2]Fraunhofer Institute of Material and Beam Technology, Winterbergstraße 28, 01277 Dresden, Germany

E-mail: achim.mahrle@iws.fraunhofer.de

Abstract. Experimental and theoretical investigations on fibre-laser assisted plasma arc welding (LAPW) have been performed. Welding experiments were carried out on aluminium and steel sheets. In case of a highly focused laser beam and a separate arrangement of plasma torch and laser beam, high-speed video recordings of the plasma arc and corresponding measurements of the time-dependent arc voltage revealed differences in the process behaviour for both materials. In case of aluminium welding, a sharp decline in arc voltage and stabilization and guiding of the anodic arc root was observed whereas in steel welding the arc voltage was slightly increased after the laser beam was switched on. However, significant improvement of the melting efficiency with the combined action of plasma arc and laser beam was achieved for both types of material. Theoretical results of additional numerical simulations of the arc behaviour suggest that the properties of the arc plasma are mainly influenced not by a direct interaction with the laser radiation but by the laser induced evaporation of metal. Arc stabilization with increased current densities is predicted for moderate rates of evaporated metal only whereas metal vapour rates above a certain threshold causes a destabilization of the arc and reduced current densities along the arc axis.

1. Introduction

Hybrid welding methods which combine two or even more different welding heat sources increasingly gain importance for the solution of specific joining tasks. The most proven methods comprise laser-arc combinations. In the majority of applications, a high power laser beam works as the primary heat source enabling a deep penetration welding process at high travel rates. The arc as the secondary heat source is applied in order to overcome some limitations of the laser welding process. As a result, hybrid laser-arc processes offer a higher gap bridging capability, an improved process performance and the possibility of a metallurgical manipulation of the weld by addition of filler metal. Extended overviews on the benefits and characteristics of hybrid laser-arc welding were among others given by Seyffarth and Krivtsun [1], Bagger and Olsen [2], Mahrle and Beyer [3] and Olsen [4].

Otherwise, the practical experience has also shown that the performance of arc welding can benefit from an additional low-power laser beam. The corresponding processes are referred to as laser-supported or laser-assisted arc welding methods which use the welding arc as the primary and the laser beam as the secondary heat source. Since the initial investigations on hybrid laser-arc welding, performed by Steen and Eboo [5-7], it is well known that synergetic effects between the arc plasma and the laser radiation occur. In case of the applied combination of a gas-tungsten arc (GTA) or tungsten inert gas arc (TIG arc), respectively, and a 2 kW CO_2 laser beam with a wavelength of λ_{CO2} = 10.6 µm, Steen and Eboo found out, that the arc preferred to root at the laser/workpiece interaction zone and that the laser beam is capable of stabilizing the plasma arc

column and reducing its resistance. It was concluded that the presence of the laser induced plasma is likely to cause a contraction of the anodic arc root and that considerable penetration of the keyhole by the arc is probable. As a consequence, the arc energy is being used more efficiently and an improved process performance can be achieved.

Subsequent investigations on the interaction phenomena between a CO_2 laser beam and a TIG arc were presented by Cui et al. [8-9], Decker at al. [10] and Finke et al. [11]. For aluminium welding they also observed a constriction of the arc, a stabilization of the anodic arc root and a reduction of the arc voltage under the influence of the superimposed laser beam. The current density of the laser-augmented arc was measured to be around fivefold higher than the current density of the single arc. The laser-supported effects were achieved for output powers in the range of 100 to 500 W with focal laser intensities between 1 and $3 \cdot 10^{10}$ W m^{-2}. In contrast to the argumentation of Steen, the mentioned authors suppose that the electron densities and temperatures within the arc column are too low for a significant direct absorption of laser radiation. Instead, Decker et al. [10] assume that the influencing of the arc behaviour by laser radiation must be primarily base on an indirect interaction as a result of the laser-induced evaporation of weld metal. The generated metal vapour is likely to ionize more than the usually applied shielding gases argon or helium and thus offers a region with improved electrical conductivity. Benefits of the laser-supported action were reported for welding steel and aluminium sheets, as well. However, in case of steel welding, substantial advantages were limited to welding regimes with increased arc lengths. Under these conditions, the anodic arc root was constricted and, as a result, increased penetration depths were achieved as demonstrated by Finke et al. [11].

Beyer et al. [12] applied for the first time a Nd:YAG laser beam for hybrid welding in combination with a TIG arc. Nd:YAG laser radiation offers a tenfold shorter wavelength of $\lambda_{YAG} = 1.06$ µm in comparison to CO_2 laser radiation. Because the absorption coefficient of gaseous components in the laser-material interaction zone is approximately proportional to the square of the laser wavelength, the plasma formation is generally much more uncritical in such a wavelength area and can be neglected under usual welding conditions. It was found out that the arc plasma burned down into the laser induced keyhole in the case of steel welding. Consequently, the seam width was not only increased at the surface but also at the root of the seam.

Stabilizing effects on TIG arcs by Nd:YAG laser radiation were reported by Hu and Ouden [13]. Measurements of the beam absorption during its travelling through the arc plasma revealed that only 1% of the incident laser power was directly absorbed. Thus, it was consequently concluded by the authors that the stabilizing effect must be basically caused by changes of the plasma arc composition as a result of the laser-induced evaporation of workpiece metal. Results of spectroscopic measurements have demonstrated that in case of the combined laser-arc process the amount of Fe ions is much higher than in pure TIG welding. Hu and Ouden concluded that the metal atoms, which offer a lower ionization potential than the applied shielding gas components, provide a more conductive stable plasma channel for arc root and column that is more capable of overcoming disturbing external forces. In case of mild steel welding benefits of the laser-supported arc welding process were demonstrated for bead-on-plate welding at low welding currents, bead-on-plate welding under asymmetrical magnetic field conditions, and welding of corner joints.

Hermsdorf et al. [14], Stute et al. [15] and Kling et al. [16] also performed welding experiments with short-wavelength laser systems such as Nd:YAG and diode lasers and reported that the laser radiation is capable of stabilizing the arc and strengthening the energy transfer from the arc into the workpiece for TIG and Gas Metal Arc (GMA) welding, as well. They stated that laser systems with short emission wavelengths induce the opto-galvanic effect in interaction with the electric welding arc. Such an effect is assumed to arise in laser-guided arc welding if the photon energy of the laser radiation matches the gap between two energy levels of the particular atoms being present within the arc column. It is stated that such an effect consequently changes the population density of the excited states of the atoms, which results in a change of the arc discharge characteristics. Only 10 to 20% of the total amount of the delivered welding power is required from the laser beam to achieve positive effects with regard to the performance capabilities of the arc welding process.

Besides stabilization and guiding of the arc, an increase of the welding speed of up to 40% at a similar penetration depth was reached for bead-on-plate welds in hard metal samples by the use of diode lasers with an emission wavelength of λ_{Diode} = 808 nm. It was found out that the benefits of the combined laser arc action were more pronounced for slightly defocused laser beams.

Up to date, most of the work on laser supported arc welding was concentrated on non-constricted free-burning arcs and only a few investigations were performed on laser supported plasma arc welding. Plasma Arc Welding (PAW) is similar to TIG welding as it also employs a nonconsumable tungsten electrode to produce an arc to a workpiece but in contrast to TIG welding a converging action of inert gas at an orifice in the nozzle of the plasma welding torch considerably constricts the arc, resulting in several advantages over the common TIG welding process. Among others, these advantages include a higher energy density, improved arc stability and a deeper penetration capability [17]. Investigations on laser augmented plasma arc welding were already presented by Walduck and Biffin [18]. They applied a 400 W continuous wave CO_2 laser in combination with a standard plasma welding power supply and torch. The investigations have been confined to the production of full penetration butt and bead-on-plate welds in different thin sheet metals with thicknesses of between 0.5 and 1.0 mm. The experimental results show that the combined action of the laser beam and plasma arc has an apparent synergistic effect, producing a larger volume of molten weld pool than the sum of the two processes separately. In case of steel welding, the achievable travel speed was increased two to three times of the laser alone. In case of aluminium, full penetration butt welds were obtained in 0.6 mm sheets with laser supported plasma arc welding whereas with the plasma arc alone, welding was prevented because a stable anode spot could not be established on the work surface. It was also noted that during PLAW the plasma arc rooted to the hot spot created by the laser beam.

Experimental results on laser assisted plasma arc welding were also presented by Fuerschbach [19]. Fuerschbach combined a 400 W pulsed Nd:YAG laser beam with a conventional plasma arc torch in a coaxial arrangement. Benefits were particularly achieved for welding aluminium alloys 6061 and 6111. The hybrid process caused fusion zones that were substantially deeper and larger than laser welds alone and enabled unique weld geometries. Furthermore, solidification cracking in the fusion zone was eliminated and the hybrid process was marginally successful in removing the tenacious oxide layer that covers aluminium surfaces. In case of weld trials on steel alloys, it was found out that in some instances the hybrid process may create conditions more favourable to keyhole mode penetration and that the arc can penetrate much deeper into the weldment with the addition of the laser beam. Consequently, the penetration depth obtained with the hybrid process was much deeper than either the arc or laser beam could solely achieve. It is interesting to note that comparative weld trials with a more focused continuous wave CO_2 laser have not shown any synergistic increases in melting capability. It was supposed that absorption and defocusing of the laser beam in the coaxial arc plasma is indicated.

So far, it can be concluded that several benefits with regard to the performance of arc welding processes can be expected by the combination with a low power laser beam. This fact motivated own investigations on laser assisted plasma arc welding. In contrast to the discussed preceding investigations, the particular feature of the applied experimental setup was the use of a highly focused single-mode fibre laser offering higher focal intensities at moderate output powers than the laser sources used before. Both experimental and theoretical investigations were carried out revealing new insights into the complex physical relationships being present in combined laser-arc processes.

2. Experimental Set-up

Experimental investigations were performed with a separate off-axis arrangement of a laser beam and a plasma arc. The experimental set-up consisting of the laser beam focusing optics, the plasma torch and measuring technique for observations of the process behaviour by high-speed video recordings is shown in figure 1. The applied laser source was a single mode (SM) fibre laser YLR-1000 SM (IPG Photonics) with a maximum output power of P_L = 1000 W and an emission

wavelength of λ_{Yb} = 1.07 µm. The nearly diffraction-limited laser beam possesses a beam parameter product of BPP < 0.34 mm mrad^{-1}. The realized focus diameter corresponds to a value of d_0 = 40 µm with a Gaussian-shaped intensity distribution (TEM_{00}-mode). With regard to the available laser power, maximum focus intensities of up to $I_{MAX} = 1.6 \cdot 10^{12}$ W m^{-2} could be realised which can be considered as being much higher than those achieved with CO_2 or Nd:YAG lasers in previous studies on laser-supported arc welding. The electric arc was generated by using the power source Tetrix 400 Plasma (EWM) in combination with the plasma torch Abiplas Weld 150 W MT (Abicor Binzel). Only the direct current electrode negative polarity (DCEN) mode being the most common current mode in TIG and plasma arc welding was considered during the experimental welding trials. In this mode, the tungsten electrode acts as a cathode, whereas the workpiece or weldment is connected to the positive pole of the power supply. Argon with a purity of > 99.996 % was applied as both shielding and plasma gas at flow rates of between 10 and 12 l min^{-1} for shielding and of between 0.5 and 0.7 l min^{-1} as plasma gas. If not otherwise stated, all of the arc welding processes were performed with a nominal arc amperage of 100 A. At this current, the plasma arc is commonly operating in the melt-in mode with moderate penetration depths only. The measured arc voltages depend on the material type being welded but were typically in the range of between 20 and 30 V. As a result, the arc power was in the order of between 2 and 3 kW. Thus, the ratio of arc power to laser beam power typically amounts values of between 3 and 8 for the most applied laser power levels of 400 – 600 watts.

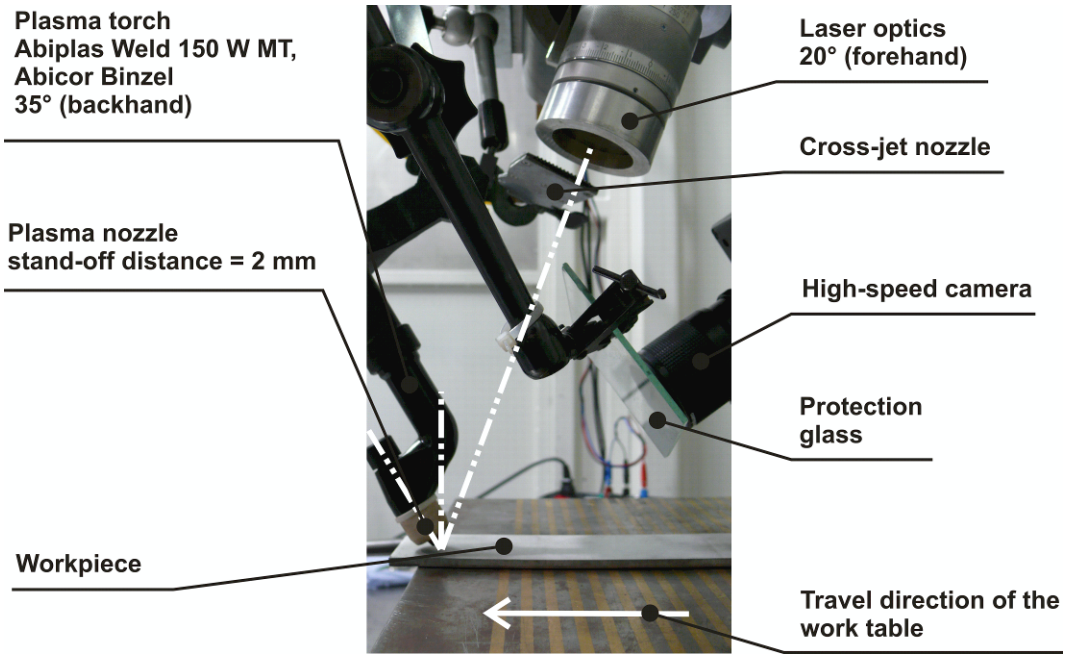

Figure 1. Experimental set-up with separate arrangement of plasma torch and laser beam.

The axis of the tungsten electrode of a plasma welding torch and the laser beam axis as well are perpendicularly oriented to the weldment for usual welding operations. However, due to the separate arrangement of both heat sources, a compromise with inclined axes had to be found in order to accomplish a common operating point. It could be shown in pilot tests that the plasma arc possesses more stability in a backhand configuration. In such an arrangement, inclination angles of between 30 and 40° could be realized without losing the stability of the arc. The laser beam was consequently oriented in a forehand configuration. The inclination angles of plasma torch and laser

beam were finally determined in such a way that a common operating point results. Process observations were enabled by means of high-speed camera recordings with a spatial resolution of 512 x 512 pixels at frame rates of 2000 Hz. Simultaneously, the arc voltage and amperage were recorded by use of the signal conditioning reck Dewetron 30-8. This measuring technique allowed the synchronous observation of the arc column and the arc characteristics in both a qualitative and quantitative way with and without the influence of an additional laser beam.

3. Experimental Results

With respect to the presented findings of the previously published work on laser-supported arc welding methods the experimental programme was subdivided into three main stages each with a particular purpose. The first welding trials were intended to demonstrate the melting capabilities of the realised plasma-arc laser-beam combination on different materials. The experiments of the second stage were focussed on measurements of the arc voltage as a function of material and beam properties. Finally, the capability of using a laser beam to stabilise the arc column as well as the possibilities of guiding the arc along a laser-defined welding path were investigated.

The welding performance of the combined laser-arc source in comparison to the single processes was investigated on different steels and aluminium alloys. The most distinctive feature of the produced weld seams was the fact of a noticeable increase in the amount of molten material of the laser-arc process. Consequently, the fact of improved process efficiency can be also confirmed in case of the combination of a highly-focused fibre laser beam and a constricted plasma arc. Resultant cross-sections of generated weld seams are exemplarily shown in figure 2 for mild steel S235JR (ASTM A284), stainless steel X5CrNi1810 (AISI 304) and aluminium alloy AlSi1MgMn (Aluminium 6082).

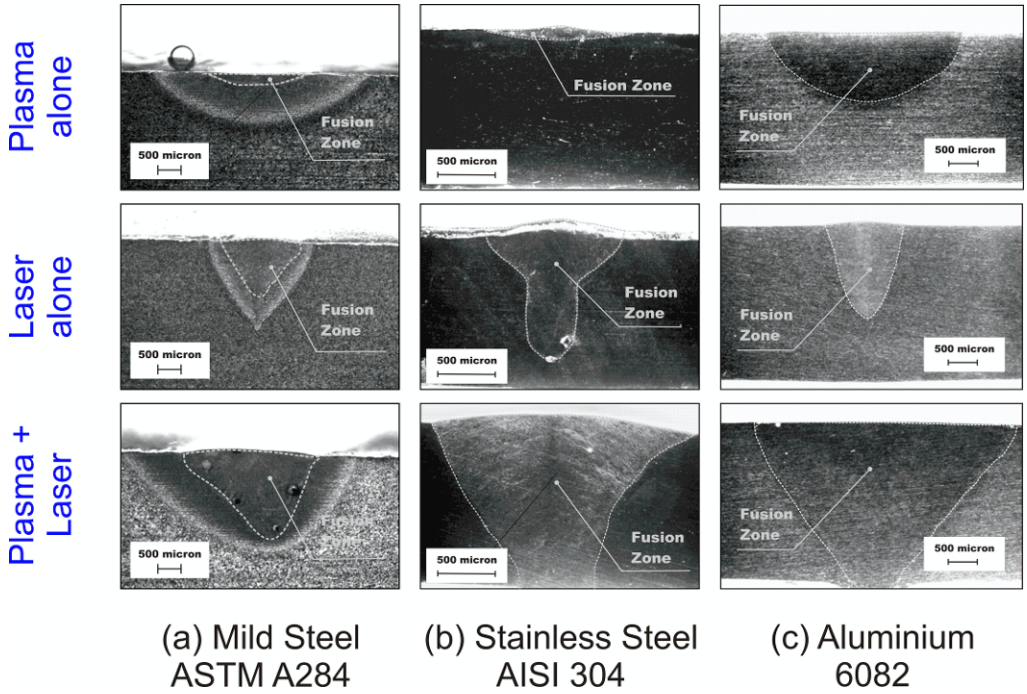

Figure 2. Weld seam cross sections of plasma, laser and laser-assisted plasma bead-on-plate welds in different base materials at 600 W laser power and 100 A arc current. (a) ASTM A284 mild steel, 10 mm thickness, 0.5 m min^{-1} welding speed. (b) AISI 304 stainless steel, 1.5 mm thickness, 1.5 m min^{-1} welding speed. (c) Aluminium alloy 6082, 2.5 mm thickness, 1.5 m min^{-1} welding speed.

At the given process parameters plasma arc welding mild or stainless steel was only capable of producing very swallow welds whereas laser welding of these materials clearly shows features of the deep penetration or keyhole effect. In case of the combined process the penetration depth is noticeably increased and the seam width is broadened not only in the upper region but over the whole thickness of the steel sheet. Considering that the single laser process was obviously acting in the deep penetration mode with a resultant high degree of energy coupling due to the possibility of multiple reflections within the characteristic vapour keyhole, the gain in process efficiency of the combined process must be primary result from an improved consumption and/or utilization of the arc energy. Similar findings were made in welding aluminium alloys. Despite the fusion zone of the pure arc welding process is more pronounced than in steel welding, probably caused by the lower melting point of aluminium, the laser-arc combination gives rise to a substantially changed weld seam geometry with increased amounts of penetration depth and seam width. In trying to quantify the observed effects, the achievable increase in welding efficiency of the laser-arc combination in comparison to the single processes was determined. In general, the welding efficiency η_W can be defined as the ratio of the theoretical amount of power P_{FZ} needed to melt the material of the fusion zone (index FZ) to the overall supplied welding power P_W according to

$$\eta_W = \frac{P_{FZ}}{P_W} = \frac{\rho \cdot w_{ch} \cdot A_{FZ} \cdot \Delta h_{FZ}}{P_W} \tag{1}$$

where ρ is the mass density of the material being welded, w_{ch} the travel speed, A_{FZ} the cross-sectional area of the fusion zone and Δh_{FZ} the required increase in specific enthalpy to cause melting. Relationship (1) can be considered as a base for a definition of a relative welding efficiency that compares the efficiency of the combined laser-arc process with that of the single processes. One gets:

$$\eta_{rel} = \frac{\eta_{PL}}{\eta_{P+L}} = \frac{\rho \cdot A_{FZ,PL} \cdot \Delta h_{FZ} \cdot w_{ch}}{P_P + P_L} \cdot \frac{P_P + P_L}{\rho \cdot \left(A_{FZ,P} + A_{FZ,L} \right) \cdot \Delta h_{FZ} \cdot w_{ch}} = \frac{A_{FZ,PL}}{A_{FZ,P} + A_{FZ,L}} \tag{2}$$

In this relation, $A_{FZ,PL}$ denotes the cross-sectional area of the combined laser-arc process, and $A_{FZ,P}$ and $A_{FZ,L}$ are the cross-sectional areas of the separately performed plasma arc and laser beam welding processes. Calculated values of measured cross-sectional areas and corresponding relative efficiencies are summarized in table 1 for the investigated materials mild steel, stainless steel and aluminium alloy 6082.

Table 1. Weld seam cross-sectional areas A_{FZ} and resultant relative welding η_{rel} efficiencies of plasma, laser and laser-assisted plasma bead-on-plate welds in different base materials at 600 W laser power and 100 A arc current. (a) ASTM A284 mild steel, 10 mm thickness, 0.5 m min^{-1} welding speed. (b) AISI 304 stainless steel, 1.5 mm thickness, 1.5 m min^{-1} welding speed. (c) Aluminium alloy 6082, 2.5 mm thickness, 1.5 m min^{-1} welding speed.

Material	$A_{FZ,P}$ / mm^2	$A_{FZ,L}$ / mm^2	$A_{FZ,PL}$ / mm^2	η_{rel} / -
Mild steel ASTM A284	0.4	1.5	3.3	1.74
Stainless steel AISI 304	0.1	0.7	1.9	2.38
Aluminum alloy 6082	2.2	1.8	6.0	1.50

The reasons for the achievable gain in process efficiency of laser-supported arc welding in comparison to the single processes are not really obvious. With respect to the results and chains of

reasoning of the published work on this topic, the next stage of subsequent investigations was focused on the determination of measurable quantities of the arc characteristics involving high-speed observations of the arc shape under the influence of an additional laser beam and corresponding measurements of the arc voltage. Particularly, the outcomes of the arc voltage revealed distinctive differences in the process characteristics between welding ferrous alloys on the one hand and welding aluminium on the other. The most characteristic results are summarised in Figure 3. In case of aluminium welding a marked drop in arc voltage in the range of between – 2 and -3 V was achieved by switching on the laser beam whereas in steel welding under the same conditions of a highly-focused laser beam generally a moderate increase in arc voltage of between 0.15 and 0.6 V was detected.

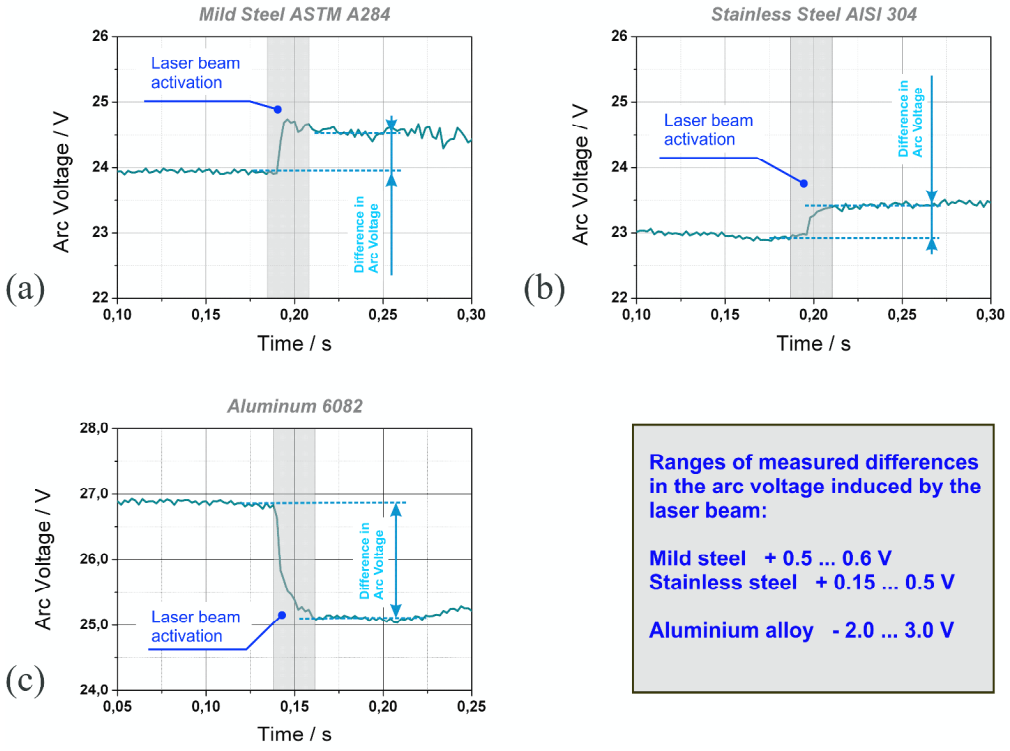

Figure 3. Arc voltage as a function of time during the activation phase of the laser beam for bead-on-plate welds in different base materials at 600 W laser power and 100 A arc current. (a) ASTM A284 mild steel, 10 mm thickness, 0.5 m min^{-1} welding speed. (b) AISI 304 stainless steel, 1.5 mm thickness, 1.5 m min^{-1} welding speed. (c) Aluminium alloy 6082, 2.5 mm thickness, 1.5 m min^{-1} welding speed.

The increase in arc voltage after switching on the laser beam during welding ferrous alloys was accompanied by a more irregular arc voltage signal and it could not be proven any beneficial effects of the laser radiation on the arc characteristics. Consequently, the phenomenon of a stabilising action of the laser radiation, as observed by Hu and Ouden [13] in case of welding mild steel with a TIG arc – Nd:YAG laser beam combination, cannot be confirmed under the conditions of a highly focused fibre laser beam and a plasma arc as realised in our own investigations. On the other hand, stabilising effects are clearly achieved in case of aluminium welding. Such a material-dependent characteristics of laser-arc processing is consistent to the observations of Maier et al. [20-21] who combined a Nd:YAG laser beam with a TIG arc. The corresponding investigations showed a pronounced fixation of the arc root also in aluminium welding only. The underlying physical effect was explained by the local laser-induced destruction of the thin oxide layer by

which aluminium surfaces are covered. This electrically insulating and high-fusing surface layer is considered as a high electrical resistance and it was assumed that the arc is going to root in locations without this high surface resistivity. A clear drop of the arc voltage as a result of the laser beam action was also proved in agreement to our investigations. In contrast to these results for aluminium welding, Maier observed no stabilising effects on the arc column in steel welding. In that case, the arc column was even clearly deflected from the laser-material interaction zone.

Additional welding experiments on aluminium test specimens were performed with the aim to quantify the laser-induced effect on the arc voltage drop. The particular material used for these experiments was the aluminium alloy AlMg3.5 (aluminium 5154) with a sheet thickness of 5 mm. At constant values of arc current (100 A) and welding speed (1 m min^{-1}) the intensity of the incident laser beam was varied as a function of laser power and beam radius as well. Within the investigated parameter range only bead-on-plate welds with partial penetration were realised. Thus, any influence of the measured data due to a transition of partial to full penetration can be concluded. Figure 4 shows the results of the conducted experimental trials.

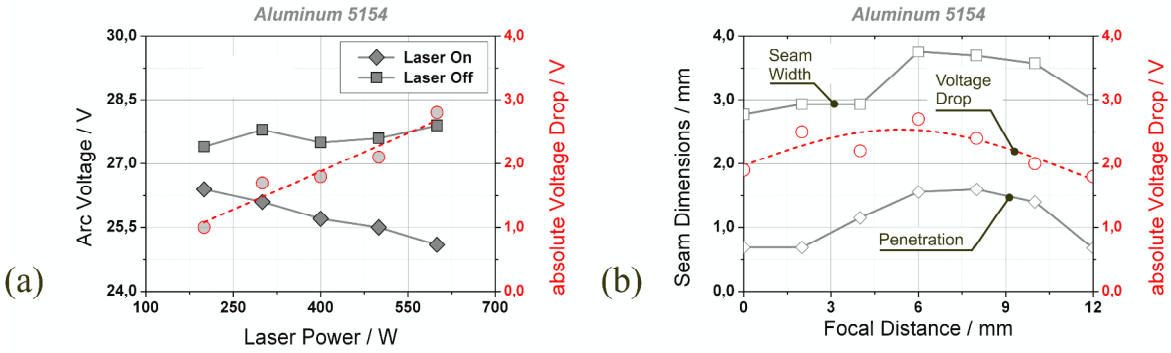

Figure 4. Laser-supported plasma arc welding of aluminium 5154. (a) Arc voltage and arc voltage drop as a function of laser power (arc current = 100 A, travel speed = 1.0 m min^{-1}). (b) Weld seam dimensions and arc voltage drop versus focal distance (arc current = 100 A, laser power = 400 W, travel speed = 1.0 m min^{-1}).

It is obvious that the drop in arc voltage after turning on the laser beam clearly depends on the applied laser power. The arc voltage decreases almost linearly with increased laser power levels within the considered range of between 200 and 600 W, see Figure 4a. The measured absolute voltage drop at 600 W laser power amounts 2.8 V and lies in the same order as the voltage drops typically measured during welding aluminium 6062. Consequently, the specific composition of a particular aluminium alloy as well as the material thickness does not seem to have a crucial impact on the phenomenon of the arc voltage drop in aluminium welding. However, stronger variations of the beam intensity by displacements of the focal plane above the surface of the workpiece being welded revealed that the achievable voltage drop must not considered in general as being proportional to the beam intensity. Figure 4b shows results of corresponding investigations with a gradual defocusing of the laser beam at a constant laser power of 400 W as a function of the focal distance, i.e. the distance between the nominal focal plane and the surface of the workpiece. The achievable voltage drop consequently shows a maximum at a particular focus intensity with a resultant increasing characteristic before and a decreasing characteristic behind this optimum. Despite the differences in the arc voltage drop within the range of between 2 and 3 V are not really exciting, a noticeable impact on the achievable process efficiency results. According to the measured data shown in figure 4b the maximum in voltage drop approximately correlates with the achievable maximum values of penetration depth and seam width, respectively. Furthermore, it can be stated that the optimisation of the investigated process always needs a careful determination of beam power and intensity.

Besides the gain in process efficiency and the marked drop of arc voltage also stabilization and guiding effects of the laser beam on the plasma arc column were observed in welding aluminium alloys. Under conditions of welding aluminium the inclined arrangement of the plasma torch gave sometimes rise to the appearance of two coexistent discharge paths with corresponding arc roots, one along to the extended torch axis (referred to as leading arc) and the other (trailing arc) perpendicularly to the surface of the workpiece being welded which gives the shortest arc length between the orifice of the torch and the workpiece. Pictures (inverted and graduated) of the arc shape extracted from high-speed video recordings during welding aluminium alloy 5154 are shown in figure 5. The trailing arc root was established just after the ignition of the arc and can be considered as the primary discharge path under conditions of a cold workpiece, see figure 5a (Regime I). The second arc root along the torch axis was formed during the course of welding, probably caused by the temperature rise of the surrounding base material and an additional support of the forced plasma stream (Regime II). Both discharge paths were competing to each other under the conditions of moderate arc currents, see figure 5b, producing irregular weld seams and variations of the arc voltage, see figure 5d. By switching on the laser beam which was focused onto the region of the leading arc root point, the trailing discharge path could be completely suppressed, see Figure 5c, and, as a result, the arc voltage was substantially lowered after a short start-up phase (Regime III).

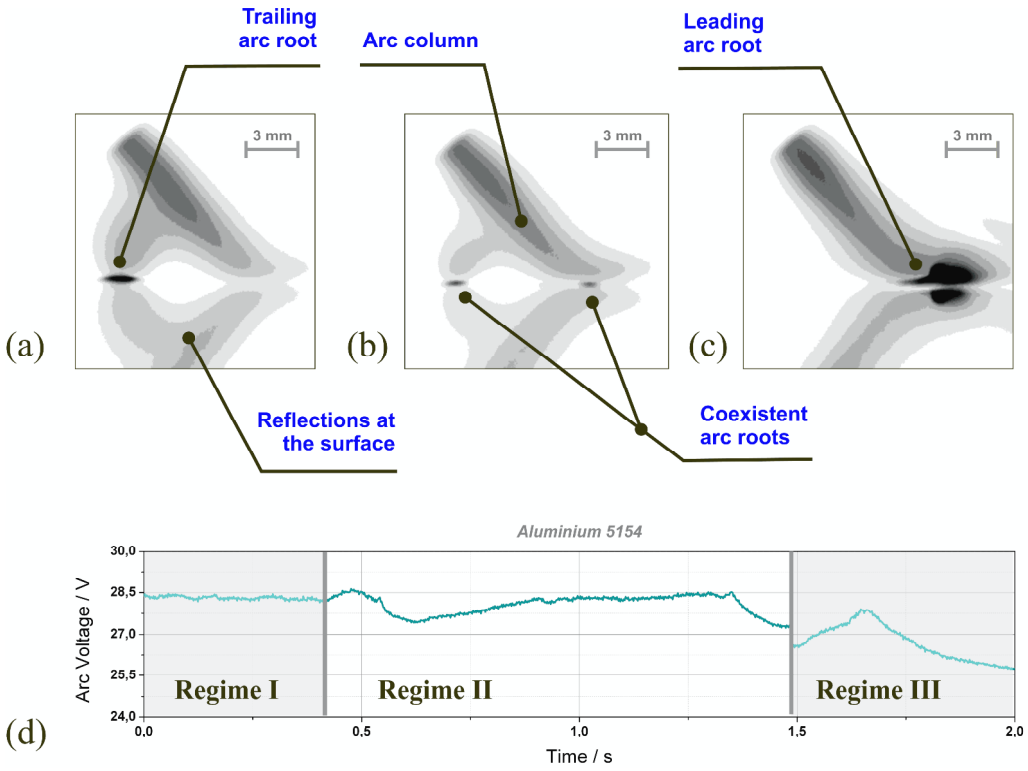

Figure 5. Arc behaviour during plasma arc welding aluminium alloy 5154 without and with laser beam support. Process parameters: Arc current = 100 A, laser power = 400 W, welding speed = 1 m min^{-1}. (a) Regime I: Formation of a trailing arc root under conditions of a cold sheet without laser beam support. (b) Regime II: Coexistent trailing and leading arc root under conditions of a heated sheet without laser beam support. (c) Regime III: Stabilization of the leading arc root with simultaneous suppression of the trailing arc root by laser beam support. (d) Corresponding data of the arc voltage as a function of time.

The stabilising effect of the laser beam on the arc root during welding aluminium alloys was utilised in final test series to guide the arc along a modified laser beam route defined by transversal oscillations of the beam spot with respect to the straightforward pass of the plasma torch. Experimental trials on aluminium alloy 5154 have demonstrated that the arc is capable of following such beam spot deflections up to distances in the order of some mm amplitude even at low laser power levels. Figure 6a shows the corresponding appearance of the surface of the weld seam for that particular case and it is worth-mentioning that the arc can be deflected from its actual weld path (corresponding to the motion of the plasma torch) with a distance which obviously outreaches its own root diameter. The arc is capable of following the laser beam spot even in case of sudden changes of the spot position. Figure 6b exemplarily shows the surface appearance for a rectangular beam oscillation during welding aluminium alloy 6082. Displacements of the root centre of up to 2 mm were achieved without loosing the stability of the arc. It is assumed that the guiding effect does not depend upon the particular composition and will be observable in any type of aluminium alloys. Furthermore, the described guiding effect can be achieved in a large range of laser beam, arc and processing parameters.

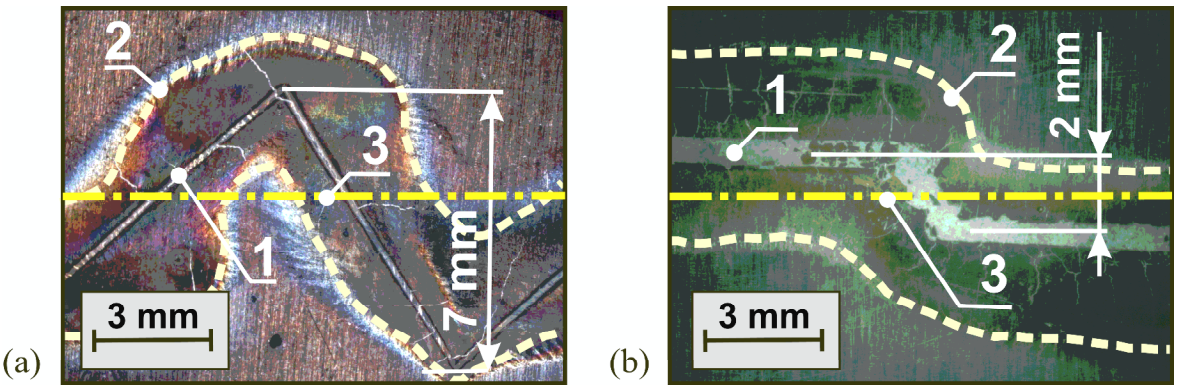

Figure 6: Arc-guiding by laser radiation (1 … weld path defined by the laser beam, 2 … boundary of the arc-generated melt track, 3 … weld path defined by the arc torch movement). (a) Laser-supported plasma arc welding of aluminium 5154 (arc current = 100 A, laser power = 80 W, welding speed = 1 m min^{-1}, transversal triangular oscillations of the laser beam with 3.5 mm amplitude at 1.5 Hz). (b) Laser-supported plasma arc welding of aluminium 6082 (arc current = 100 A, laser power = 600 W, welding speed = 1.5 m min^{-1}, transversal rectangular oscillations of the laser beam with 1 mm amplitude at 0.5 Hz)

4. Numerical analysis of particular laser-arc interaction phenomena

To further the understanding of laser-arc processing also theoretical investigations have been performed involving the numerical simulation of the plasma arc and its possible interaction with laser radiation. The main purpose of the corresponding analysis was the evaluation of the various hypotheses about the relevant interaction mechanisms that may be important for the considered process of laser-supported arc welding. Three different phenomena and their specific impact on the arc characteristics were investigated in detail, namely (i) the laser-induced evaporation of base-material, (ii) the direct absorption of laser radiation by the arc plasma and (iii) the additional heating of the surface of the workpiece by the laser beam. In order to get clear hypotheses about the particular impact and relevance of each individual effect, the considered phenomena were analysed in a separate manner without consideration of any cross-effects and without taking into consideration the formation and the behaviour of the generated melt pool. The simulation was consequently focussed on the analysis of the arc plasma. In that case, the impact of the relative

motion between arc and workpiece on the shape of the arc column could be neglected and the simulation was performed under axisymmetrical conditions.

The analysis was performed by means of a magneto-hydrodynamic arc model previously developed by Schnick et al. [22-24]. This model was originally applied for the simulation of the arc behaviour during pure arc welding processes such as tungsten inert-gas (TIG) and gas metal-arc (GMA) welding and implemented using the commercial software package Ansys CFX. Besides the coupled phenomena of heat, mass and momentum transfer within the arc column also the relevant electromagnetic and radiative effects, the characteristic processes of the sheath regions close to the electrodes and demixing effects between different components of the arc plasma as in case of mixtures of shielding/plasma gas and metal vapour are taken into account. As a result, the distribution of temperature, velocity, electric potential and current density as well as magnetic induction, resistive heating and Lorentz forces can be calculated under the conditions of a local thermodynamic equilibrium plasma (LTE approach), i.e. the corresponding plasma properties are regarded as a function of temperature and composition only. The thermodynamic properties were calculated according to the data given by Murphy [25] for a temperature range of between 300 and 30000 K. Radiative effects are considered by use of the net emission coefficient (NEC) model. Reliable NEC data are available for argon [26] and iron vapour [27] as well. For mixtures of both species, the net emission coefficient can be determined as a mole-fraction weighted average as recommended by Cressault et al. [28].

As a result of previous studies on laser-arc processes it was stated by different authors that the occurrence of laser-induced metal vapour is likely to have a noticeable positive effect on the arc stability. Such an explanation seemed to be very reasonable due to the fact of the low ionisation potential of metal atoms in comparison to the usually applied plasma and shielding gases such as argon and helium, and it was concluded that the easy-to-ionize metal atoms offer a preferred discharge path with high electric conductivity enabling a constriction and focusing of the arc. In order to verify such a thesis, the arc behaviour under the influence of metal vapour was simulated by taking the example of iron vapour – argon mixtures for which the required properties are currently available. The metal vapour in laser beam – arc combinations does preferably occur as a consequence of the laser-induced evaporation of base material in combination with the deep penetration or keyhole effect. The metal vapour flows out of the vapour capillary at usually high velocities. Theoretical estimations of the vapour velocities above the keyhole resulted in values of several hundred meters per second dependent upon the effectively absorbed laser intensity in case of welding ferrous alloys [29]. The effect of the resultant inflow of iron vapour into the arc plasma was considered in the form of a corresponding boundary condition. For that purpose an orifice at the modelled surface domain of the workpiece was considered. This orifice was assumed to possess the same diameter as the laser beam and enabled the specification of the inflow velocity of the metal vapour. Figure 7 shows computed distributions of temperature and Fe-mass fraction for a moderate inflow of metal vapour at 100 m s^{-1} (LV arc according to Figure 7a) and for a high vapour rate of 600 m s^{-1} (HV arc according to Figure 7b). The impact of the metal vapour on the arc characteristics is clearly obvious. At first glance, the most distinctive feature between the two simulation examples is the apparent constriction of the arc in case of the high metal vapour rate but this constriction of the arc shape does not cause higher thermal core intensities of the arc. In contrast and with respect to the computed temperature distribution in both examples, the overall energy content of the HV arc seems to be even smaller than in case of the LV arc. The reason of this phenomenon is that metal vapour is preferably accumulated in the fringe of the arc due to demixing effects and, most importantly, metal vapour possesses a considerably higher radiative emission coefficient than argon, typically in the range of two orders of magnitude [28]. The noticeably higher emission coefficient of iron vapour forces radiative losses to the environment and causes in such a way a cooling down of the arc plasma. As a result, arc regions with considerable amounts of metal vapour do typically exhibit temperatures below 5000 K whereas the argon plasma reaches maximum temperatures in the core region of the arc of between 15000 and 22000 K. The accumulation of metal vapour in the fringe of the arc was also proven by corresponding high-speed camera observations using an interference narrow-band filter centred at 520 nm and with a

bandwidth of 10 nm FWHM (Full Width at Half Maximum), see Figure 6c. Nevertheless, in case of low vapour rates, the concentration and ionisation of metal vapour atoms within the very thin transition layer between the arc plasma and the workpiece just above the keyhole causes a substantial increase of the electrical conductivity and as a result a moderate rise of the current density of approximately 10% as well as a slight decrease of the arc voltage, see Figure 7d. A highly forced stream of metal vapour at high flow velocities does however displace the hot argon plasma from the lower central region near the arc axis. In this case, the hot argon plasma regions just above the workpiece offer better capabilities for an off-axis transfer of the arc current than through the central cold metal vapour plasma region above the laser-induced keyhole. As a result, a central minimum in current density distribution is computed near the surface of the workpiece, see Figure 7d. Additionally, an increase in arc voltage was calculated under those conditions in accordance with the experimental results for welding ferrous alloys. It is assumed that the currently realised set-up with a highly focussed fibre laser beam corresponds to conditions with high vapour flow velocities due to the small focus radius and the high intensity of the laser spot. The revealed dependence of the arc behaviour on the laser-induced metal vapour rate gives furthermore good reasons for some observed effects during laser-arc welding steels. Besides the increase in arc voltage, also the observation that working with a defocused laser beam may improve the process performance of laser-arc combinations as reported by Kling et al. [16] or the fact that by use of a highly focused CO_2 laser beam no beneficial effects on the arc characteristics could be achieved as reported by Fuerschbach [19] can be considered as a confirmation of the simulation results. It is assumed that metal vapour in case of aluminium welding acts in a similar way. However, under the conditions of the same incident laser intensity, the metal vapour rates in aluminium welding are likely to be noticeably smaller in comparison to steel welding due to a higher reflectivity, more pronounced heat losses into the base material because of the high thermal conductivity of aluminium and the great range between melting and boiling point.

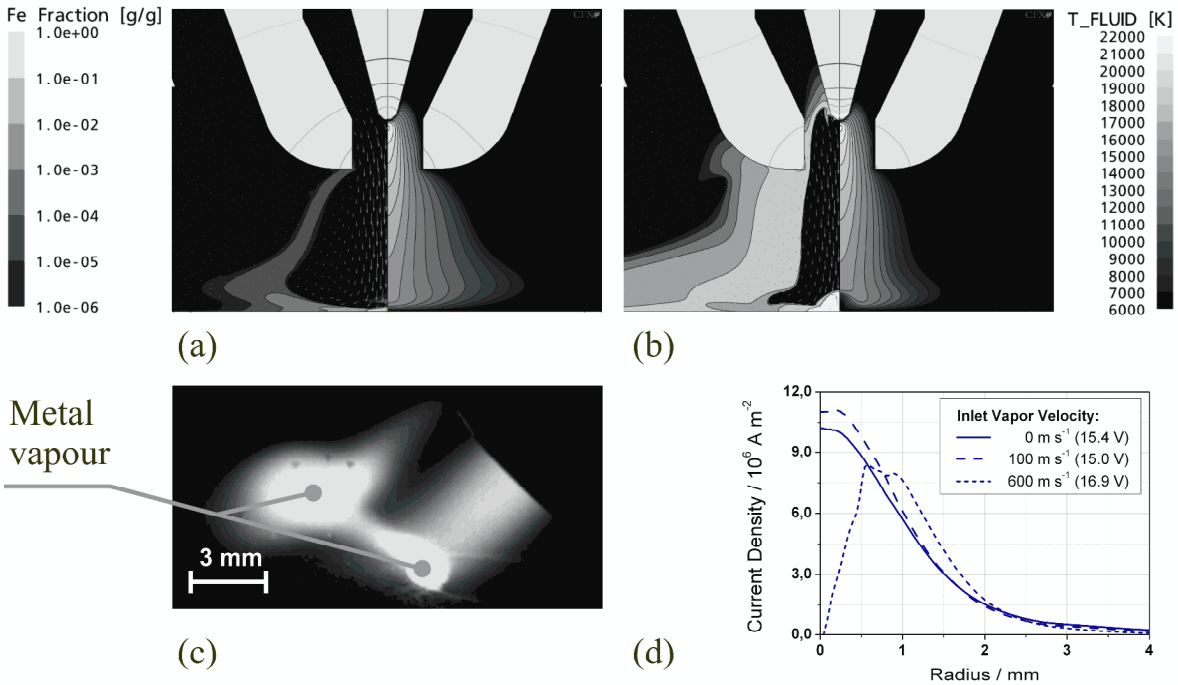

Figure 7. The influence of laser-induced evaporation of metal (iron) on the characteristics of an argon arc plasma. (a) Fe fraction and temperature distribution for a vapour inflow velocity of 100 m s^{-1}. (b) Fe fraction and temperature distribution for a vapour inflow velocity of 600 m s^{-1}. (c) Experimental high-speed observation of metal vapour. (d) Calculated current densities and arc voltages as a function of the metal vapour velocity (right).

In contrast to the complex impact of metal vapour on the arc characteristics, the direct heating of the arc plasma in interaction with the laser beam seems to play a secondary role only. In order to simulate this effect, the beam geometry was calculated as a function of the spatial coordinate in beam propagation direction and the central arc axis, respectively. Within the overlapping region of laser beam and arc, a particular amount of the incident laser power in the range of between 0 and 10% was assumed to be absorbed by the arc plasma. Resultant current densities of the arc just above the workpiece being welded are shown in Figure 8a. The calculated data demonstrate that the current density is hardly influenced by the additional heating of the arc plasma even in case of a relatively high absorption degree.

Finally, the possible influence of the thermal state of the surface being welded on the arc characteristics was investigated. For this purpose, Gaussian distributed temperature profiles $T = f(r)$ in the range of between 300 and 3000 K were set as a boundary condition for the anodic sheet region of the arc. It is assumed that this methodology can serve as a crude model of the additional heating effect of the focused laser beam if the standard deviation of the Gaussian distribution is thought to be in the range of the laser beam radius. The width of the heated zone was varied by changing the standard deviation σ with a fixed temperature maximum of T_{max} = 3000 K at r = 0. Calculated current densities and arc voltages as a function of the σ-value are shown in Figure 8b. It can be seen that the current density and the arc voltage are hardly influenced in case of small σ-values in comparison to an isothermal cold surface with a temperature of 300 K. However, for broader temperature distributions the current density is more homogeneously distributed over the affected area and the arc voltage is also decreased. With respect to the experimental findings, the last case may be appropriate to welding aluminium specimens in which the absorbed laser energy is broader distributed due to the high thermal conductivity of these materials. This effect can partially explain the measured voltage drop during welding aluminium. However, the measured values are noticeably higher than the calculated ones and this may be further an indication that also the local removal of the oxide layer probably has an additional effect on the reduction of the arc voltage as already assumed by Maier et al. [20-21].

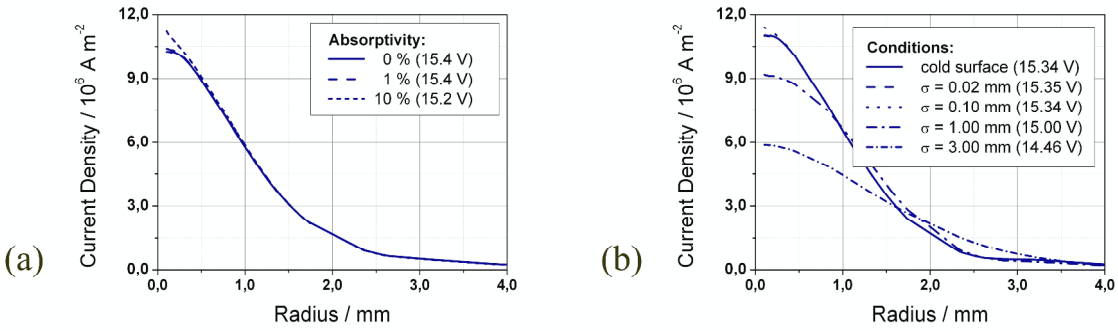

Figure 8. Current density vs. radius (distance from the arc axis) as a function of direct beam absorption (a) and with consideration of the heating of the anodic arc root by the laser beam (b).

5. Summary and Conclusions

Experimental and theoretical investigations on laser supported plasma arc welding have been carried out. The evaluation of welding experiments on different types of metallic sheets shows that the combination of a laser beam and a plasma arc offers some substantial benefits in comparison to the single processes. First of all, the melting efficiency could be noticeably increased for almost each material under investigation. Secondly, the combination of both procedures offers some potential for a purposeful shaping of the seam geometry. In case of welding aluminium alloys also a stabilization of the arc column in conjunction with a clear drop in arc voltage as well as a guiding of the anodic arc root could be proven. Instead, achieving measurable improvements of the arc

characteristics for welding ferrous alloys seems to be a more challenging task. Corresponding simulations of the arc behaviour have revealed that the laser-induced evaporation of weld metal probably exerts the most dominating influence on the arc properties. In dependence on the metal vapour rate the impact can be a negative or a positive one. High vapour rates causes an increase of the arc voltage as well as a strongly modified current transfer whereas low vapour rates seem to be serving as a stabilizing factor.

The theoretical findings may give some good reasons why beneficial effects of additional laser radiation will be almost always observable in welding aluminium alloys. In that case the evaporation rates are not so pronounced as in steel welding and the surface of the material shows a broader temperature distribution due to the high thermal conductivity. Also the local destruction of the oxide layer may exert a positive influence on the arc stability and the guidability of the arc root. In contrast, the reported contradictory observations in case of laser-supported arc welding of ferrous alloys can be ascribed to different experimental conditions with respect to the applied laser intensity. In case of strongly focused laser beams, the destabilising effects may be dominate whereas stabilising actions are probably caused under conditions of moderately defocused laser beams. It is consequently suggested that not the type or wavelength of the applied laser source is the most important factor for achievements of beneficial effects in laser-supported arc welding but the focussing conditions and the total power of the laser beam. Our findings indicate that working with a cautiously defocused laser beam spot can be a favourable choice under the conditions of laser-supported arc welding.

With respect to the results of the presented experimental and theoretical analysis, it can be clearly concluded that the gain in melting efficiency of the combined laser-arc process must not correlate with a corresponding improvement of measurable quantities of the arc characteristics. Despite the process efficiency noticeably increased for any material investigated, an enhancement of the arc stability and a guiding and fixation of the arc root was only observed for aluminium welding with the specified experimental set-up. However, this fact must not be considered as a profound mystery. As elaborated by Eagar [30] the bulk of the heat that melts the metal being welded is provided due to the flow of current into the metal and not by the heat of the arc plasma that only contributes roughly 20% of the total delivered heat. It is consequently more likely to assume that the improved melting efficiency either results from favourable changes of the current distribution across the surface of the anodic workpiece or from improved heat flow conditions inside the base material.

Acknowledgements

The authors are grateful for the financial support given by the German Research Foundation DFG within the project ‘Experimentelle und theoretische Untersuchungen zur Verfahrensoptimierung beim Wolfram-Plasmaschweißen durch Laserstrahlung geringer Leistung’, Contract No. FU 307/4-1 and BE 1875/19-1.

References

[1] Seyffarth P and Krivtsun I V 2002, *Laser-Arc Processes and their Applications in Welding and Material Treatment*, Taylor & Francis.
[2] Bagger C and Olsen F O 2005, Review of laser hybrid welding, *Journal of Laser Applications*, Vol **17**, No 1, 2-14.
[3] Mahrle A and Beyer E 2006, Hybrid laser beam welding – classification, characteristics, and applications, *Journal of Laser Applications*, Vol **18**, No 3, 169-180.
[4] Olsen F O (ed) 2009, *Hybrid Laser-Arc Welding*, Woodhead Publishing Limited.
[5] Eboo M, Steen W M and Clarke J 1978, Arc augmented laser welding, *Proc. of the Fourth Int. Conference on Advances in Welding Processes* Harrogate (UK), 257-265.
[6] Eboo M and Steen W M 1979, Arc augmented laser welding, *Metal Construction*, Vol **11**, No 7, 332-335.

[7] Steen W M 1980, Arc augmented laser processing of materials, *Journal of Applied Physics*, **51**(11), 5636-5641.
[8] Cui H, Decker I and Ruge J 1989, Wechselwirkungen zwischen WIG-Schweißlichtbogen und fokussiertem Laserstrahl, *Proc. Laser'89*, Springer Verlag, 577-81.
[9] Cui H, Decker I, Pursch H, Ruge J, Wendelstorf J and Wohlfahrt H 1992, Laserinduziertes Fokussieren des WIG-Lichtbogens, *Proc. Schweißen und Schneiden'92*, DVS-Verlag GmbH, 139-143.
[10] Decker I, Wendelstorf J and Wohlfahrt H 1995, Laserstrahl-WIG-Schweißen von Aluminiumlegierungen, *Proc. Schweißen und Schneiden'95* Dresden (Germany) DVS-Verlag GmbH, 96-99.
[11] Finke B R, Stern F and Decker I 1991, Auswirkungen eines unterstützenden Laserstrahls auf den WIG-Schweißprozess, *Proc. Strahltechnik – Beam Technolgy*, DVS-Verlag GmbH, 96-99.
[12] Beyer E, Dilthey U, Imhoff R, Maier C, Neuenhahn J and Behler K 1994, New aspects in laser welding with an increased efficiency, *Proc. ICALEO'94* Orlando (FL USA) Laser Institute of America, 183-192.
[13] Hu B and den Ouden G 2005, Laser induced stabilisation of the welding arc, *Science and Technology of Welding and Joining*, Vol **10**, No 1, 76-81.
[14] Hermsdorf J, Ostendorf A, Stahlhut C, Barroi A, Otte F and Kling R 2008, Guidance and stabilisation of electric arc welding using Nd:YAG laser radiation, *Proc. PICALO 2008*, Beijing (China) Laser Institute of America, 335-340.
[15] Stute U, Kling R and Hermsdorf J 2007, Interaction between electrical arc and Nd:YAG laser radiation, *Annals of the CIRP*, 56/1/2007, 197-200.
[16] Kling R, Otte F, Stahlhut C and Hermsdorf J 2007, Minimale Laserleistung mit Lasern angepasster Strahleigenschaften für das Laser/MSG-Hybridschweißen in Fertigungssystemen für die Fahrzeugfertigung, *Proc. Die Verbindungsspezialisten 2007*, DVS-Verlag GmbH, 409-418.
[17] Messler R W 2004, *Principles of Welding*, WILEY-VCH Verlag GmbH & Co. KGaA, 55-57.
[18] Walduck R P and Biffin J 1994, Plasma arc augmented laser welding, *Welding & Metal Fabrication*, April 1994, 172-176.
[19] Fuerschbach P W 1999, Laser assisted plasma arc welding, *Proc. ICALEO 1999*, San Diego (CA USA) Laser Institute of America, 102-109.
[20] Maier C, Beersiek J, Neuenhahn J, Behler K and Beyer E 1995, Kombiniertes Lichtbogen-Laserstrahl-Schweißverfahren – Online Prozessüberwachung, *Proc. Schweißen und Schneiden'95* Dresden (Germany) DVS-Verlag GmbH, 45-51.
[21] Maier C, Neuenhahn J, Behler K and Beyer E 1996, Laserstrahlschweißen in Kombination mit konventionellen Techniken – Hybridschweißen, *Proc. 4. Konferenz Strahltechnik* Halle (Germany): SLV Halle, 14-18.
[22] Schnick M, Füssel U and Spille-Kohoff A 2010, Numerical investigations of the influence of design parameters, gas composition and electric current in plasma arc welding (PAW), *Welding in the World*, Vol **54**, No 3-4.
[23] Schnick M, Füssel U, Hertel M, Spille-Kohoff A and Murphy A B 2010, Metal vapour causes a central minimum in arc temperature in gas-metal arc welding through increased radiative emission, *Journal of Physics D: Applied Physics*, **43**, 022001, 5 pages.
[24] Schnick M, Füssel U, Hertel M, Haessler M, Spille-Kohoff A and Murphy A B 2010, Modelling of gas-metal arc welding taking into account metal vapour, *Journal of Physics D: Applied Physics*, **43**, 434008, 11 pages.
[25] Murphy A B 2001, Thermal plasmas in gas mixtures, *Journal of Physics D: Applied Physics*, **34**, R151-R173.
[26] Evans D L and Tankin R S 1967, Measurement of emission and absorption of radiation by an argon plasma, *Physics of Fluids*, **10,** 6, 8 pages.
[27] Menart J and Malik S 2002, Net emission coefficients for argon – iron thermal plasmas, *Journal of Physics D: Applied Physics*, **35** (9), 867-874.

[28] Cressault Y, Teulet P and Gleizes A 2008, Thermal plasma properties in gas or gas-vapour mixtures, Proc. of the 17th International Conference on *Gas Discharges and Their Applications*, 7-12 Sept. 2008, Cardiff.
[29] Beyer E 1995, *Schweißen mit Laser*, Springer-Verlag, pp 60-62.
[30] Eagar T W 1990, An iconoclast's view of the physics of welding – rethinking old ideas, *Proc. Recent Trends in Welding Science and Technology*, ASM International, Materials Park, (OH, USA), 341-346.